Structure and rheology of SiO_2 nanoparticle suspensions under very high shear rates

J. Chevalier,[1] O. Tillement,[2] and F. Ayela[1,3,*]
[1]*Institut Néel, CNRS, 25 Avenue des Martyrs, BP 166, 38042 Grenoble Cedex 9, France*
[2]*Laboratoire de Physico-Chimie des Matériaux Luminescents, UCBL, 10 Rue A. M. Ampère-Bat. A. Kastler, 69622 Villeurbanne Cedex, France*
[3]*Laboratoire des Ecoulements Géophysiques et Industriels, CNRS-UJF, BP 53, 38041 Grenoble Cedex 9, France*
(Received 31 March 2009; revised manuscript received 16 September 2009; published 6 November 2009)

High shear rate experiments have been performed with capillary microviscometers onto SiO_2 nanoparticles dispersed in alcohol (so-called nanofluids). The aim of these experiments was to investigate the processes of aggregation and dislocation of the nanoparticles in a shear flow under perikinetic and orthokinetic conditions. Shear rates as high as 2×10^5 s^{-1} were obtained in pressure-driven microchannels laminar flows. All the nanofluids under test have displayed a Newtonian behavior but with a strong enhanced viscosity, that is, the consequence of an effective volume concentration higher than the real one. It was possible to determine the average size of the aggregates and to find a correlation between their structure and the range of the hydrodynamic Peclet number at which experiments were performed. These results display a strong evidence of the role of aggregates and support the recent conclusions about the controversy of the thermal properties of nanofluids.

DOI: 10.1103/PhysRevE.80.051403 PACS number(s): 83.80.Hj, 81.07.−b

I. INTRODUCTION

Nanofluids are liquids that contain a small volume fraction of nanoparticles. These substances have been prepared to improve the inherently poor thermal conductivity of heat transfer fluids. They are extremely stable and do not exhibit significant settling under static conditions. Nanofluids should take advantage of the presence of a high-thermal conductivity solid phase, even if the interface thermal resistance between nanoparticles and liquid is expected to reduce the conductivity of these mixtures.

So, nanofluids have attracted great interest due to a lot of reports of anomalous enhanced thermal properties at low volume fraction. A recent review [1] surveys most of the papers claiming unexpected experimental results. These results are joined to a great number of theoretical models devoted to give a physical explanation: Brownian motion inducing microconvection or nanoconvection, interfacial liquid layer, near field interaction between closely separated particles. No firm conclusion can be drawn from a lot of fluctuating data. Nevertheless, there is a trend to agree with the fact that aggregates play a major role because they give way to an apparent volume fraction ϕ_a higher than the real one [2,3]. Philip *et al.* observed a strong enhancement of thermal conductivity in a nanofluid containing magnetite particles, when a magnetic field was applied [4]. That was attributed to the formation of chainlike structures and was claimed to be consistent with the role of aggregates. So, the apparent failure of effective-medium theories that assume well-dispersed particles should be nothing but an artifact because such a model does not apply to clusters of nanoparticles. However, such an explanation is still under controversy [5]. For instance, a recent paper [6], supported by experiments with very dilute nanofluids, claims that models based on Brownian dynamics should be considered.

The viscosity of nanofluids has been studied to a much lesser extent compared with their thermal conductivity. However, rheological properties can provide us with the knowledge on the microstructure within the nanofluids, under both static and dynamic conditions and reveal the mechanisms of heat transfer enhancement. For applications, such as heat exchangers, the benefit from thermal-conductivity enhancement has to be balanced with the consequence of the increment of viscosity. Very few studies have been reported on the rheological behavior of nanofluids, although there is evidence of a relationship between the thermal and rheological behavior of these suspensions, and there is some inconsistency among the published studies on the rheology of nanofluids.

Most of the papers concern dilute or semidilute suspensions with a real solid volume fraction $\phi<0.1$. For these suspensions, a Newtonian behavior and a linear evolution of the dynamic viscosity with ϕ are expected. On one hand, Prasher *et al.* [7] reported experimental results on the viscosity of alumina-based nanofluids and compared the increase in the nanofluid viscosity to the enhancement in the thermal conductivity. The nanofluids under test displayed a Newtonian behavior. The authors suggested that aggregates should have a huge importance on the viscosity as for the thermal conductivity. They applied a Krieger-Dougherty model with the volume fraction of aggregates to explain the increase in viscosity. Timofeeva *et al.* [8] published large increases and size effects in viscosity for suspensions of 11, 20, and 40 nm Al_2O_3 particles dispersed either in water or ethylene glycol. The results were attributed to a dendritic agglomeration. They were correlated with relative enhancements of the thermal conductivity. Surprisingly, at a fixed volume fraction, the highest thermal conductivity was observed for the fluids with the lowest viscosity. Das *et al.* [9] characterized water based of Al_2O_3 nanoparticles. The nanofluids exhibit a Newtonian behavior with 1% and 4% particle volume concentrations. The authors did not explore the evolution of the viscosity with ϕ. Garg *et al.* [10] measured the viscosity of dilute copper-ethylene glycol nanofluids and observed a linear in-

*frederic.ayela@hmg.inpg.fr

crease in the viscosity with the volume concentration. Once again, these results are in agreement with an explanation based on the role of aggregates. Murshed *et al.* [11,12] investigated the thermal conductivity and viscosity of nanofluids. They found an anomalous increase in the viscosity of the nanofluids they tested and a discrepancy with the viscosity measurements published by other groups with similar mixtures. That was partly attributed to the difference in the size of the clusters. In conclusion of a recent paper, Chen *et al.* [13] distinguished dilute, semidilute, semiconcentrated, and concentrated nanofluids. Their conclusions support the role of aggregates. On the other hand, Tseng and Lin [14] studied TiO_2 nanoparticles dispersed in water over a range of volumetric solid concentration $0.05<\phi<0.12$ and shear rates $10<\gamma<10^3$ s^{-1}. They observed a pseudoplastic flow behavior with yield-stress values and an experimental increase in the relative viscosity as ϕ was increased. Kwak and Kim [15] studied very dilute rodlike CuO nanoparticles dispersed in ethylene glycol. Transmission electron microscopy (TEM) observations demonstrated that the particles were in an aggregate state. A non-Newtonian behavior was observed. He *et al.* [16] measured aqueous TiO_2 nanofluids and observed a shear thinning behavior until $\gamma \approx 100$ s^{-1} above which a constant viscosity is observed. The constant viscosity increases erratically with increasing volume concentration and particle diameter. The same group observed a Newtonian behavior but with ethylene glycol-based TiO_2 nanofluids and explained their rheological properties by the aggregation mechanism [17]. The discrepancy between these two results is attributed to strong interactions between the base liquid and nanoparticles. Some results concern concentrated or semiconcentrated suspensions [18–20]. The low shear limiting experimental viscosities agree with hard-sphere models, taking into account the presence of a surfactant layer or of an electric double layer around the particles.

Rheological and thermal properties of carbon nanotubes based nanofluids have been studied [21,22], but the anisotropic aspect ratio of the nanotubes and the complexity of the problem are out of the scope of this paper, which limits to spherical nanoparticles.

Keblinsky *et al.* [1] pointed out that there is a need to accurately identify the cluster configuration within the nanofluids to reach a better understanding of the transport properties of nanofluids. The present paper addresses these issues, with high shear rate experiments on nanofluids flowing through microchannels. Microfluidics in a unique experimental approach makes possible the manipulation of clusters under a unique range of strong shear rates together with a laminar flow. In the experiments presented below, the role of clusters has been clearly enhanced and it was possible to proceed up to the sizes and structures of aggregates.

The outline of this paper is as follows. In Sec. II, the mechanisms of perikinetic and orthokinetic aggregations are detailed, and the high shear rate rheology of nanosuspensions is discussed. The nanofluids under test and the experimental devices are described in Sec III. Results are presented and discussed in Sec. IV. Section V contains the conclusions.

II. PERIKINETIC AND ORTHOKINETIC AGGREGATIONS OF NANOFLUIDS

The processes of aggregation of small particles have been widely studied. Linear aggregation may take place in the presence of an intrinsic or induced dipole moment between two particles and give way to a chainlike structure [4,23]. Simulations and experimental evidences of the kinetic formation of fractal clusters, by diffusion- or reaction-limited cluster aggregation, are well established [24,25]. Perikinetic aggregation is due to Brownian motion and is relevant with nanoparticles because the average length ℓ between two neighboring particles shortens with nanofluids,

$$l = d[(\phi_m/\phi)^{1/3} - 1], \tag{1}$$

where d is the diameter of the particles, ϕ is the solid volume fraction, and ϕ_m is the crowding factor that is the maximum packing fraction. Equation (1) has been stated from a simple configuration, where nanoparticles obey a cubic arrangement. The Brownian characteristic times t_B necessary for two neighboring particles to collide is

$$t_B = \frac{3\pi\eta_0 d l^2}{4k_B T}, \tag{2}$$

where η_0 is the dynamic viscosity of the base fluid, k_B is the Boltzmann constant, and T is the temperature.

Once clusters are formed and when an equilibrium arrangement is reached, the average length between aggregates and the Brownian time increases. The motion of the particles with the fluid flow in a nonuniform field of velocity will lead to a shear thinning caused by the fact that particles will adopt a more flow oriented arrangement. At high shear rates, one expects the cluster to break up under the action of large shear stress. By increasing the shear rate, orthokinetic aggregation is then due to shear flow that tends to bring particles close each other. High applied shear stress leads to shear thickening, which is understood to be a consequence of the dominance of short-range hydrodynamic interactions. A shearing characteristic time t_γ is defined by

$$t_\gamma = \frac{1}{\gamma d}, \tag{3}$$

where γ is the shear rate.

The relative influence of perikinetic and orthokinetic aggregations can be expressed via the Peclet dimensionless number Pe. The Peclet number is defined from the ratio t_B/t_γ, that is,

$$\mathrm{Pe} = \frac{3\pi}{8}\frac{\eta_0 \gamma d^3}{k_B T}\left[\left(\frac{\phi_m}{\phi}\right)^{1/3} - 1\right]. \tag{4}$$

Pe is a number that gauges the importance of Brownian motion relative to shear forces. It takes care of the main effects of particle size, base fluid viscosity, and temperature. The arrangement of particles depends on Peclet. Figure 1 enhances the relevance of perikinetic and orthokinetic aggregations, respectively. The different situations with $\mathrm{Pe}<1$ and $\mathrm{Pe}>1$ have been largely studied with microsized particles [26]. Shear thickening flow of nanoparticle suspensions flocculated by polymer bridging has been studied recently, but at

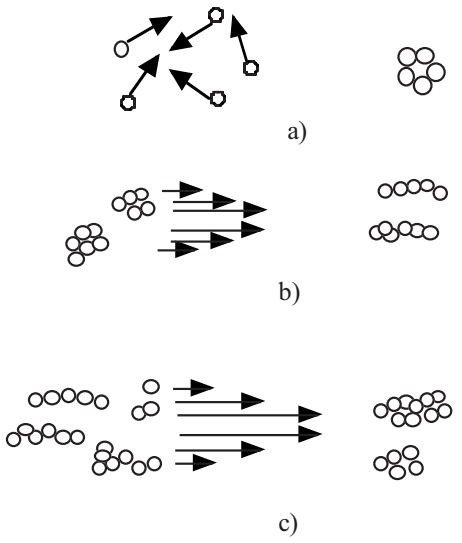

FIG. 1. Perikinetic aggregation (a) due to Brownian motion ($Pe<1$), shear thinning in a nonuniform field of velocity flow (b), and orthokinetic aggregation (c) when hydrodynamic interactions become predominant ($Pe>1$) under high shear rates. For dilute water-based nanofluids ($d=25$ nm) at ambient temperature, the transition $Pe=1$ occurs with shear rates $\gamma \approx 10^5$ s^{-1}.

shear rate values below 300 s^{-1} [27]. However, reaching high Pe values with nanoparticles in a laminar flow is an experimental challenge because of the very strong shear rates that are necessary. Such an experimental situation is hardly attainable with conventional rheometers because disturbances, such as entrance or inertial effects, viscous heating, wall slip, or transition from laminar to turbulent flow, may occur.

Microfluidics is often presented for applications, where only microliters sample volumes are available. But the benefits of microchannels do not reduce to a low consumption of fluids. From a physical and mechanical point of view, microfluidics can offer high shear rates combined with low Reynolds numbers Re and low viscous heating. Let us consider a Newtonian fluid flowing through a microchannel of height H and width $W \gg H$. To keep a laminar flow until $Re=Re_c \approx 2300$, the height H must obey

$$H < \left[\frac{8 \eta \mathrm{Re}_c}{\gamma \rho} \right]^{1/2}, \tag{5}$$

where η and ρ are the viscosity and the density of the fluid, respectively. When conventional values $\rho \approx 10^3$ kg/m^3 and $\eta \approx 1$ mPa s are used, one finds that a laminar flow can sustain at $\gamma \approx 10^6$ s^{-1} only when $H<135$ μm. High shear microfluidics was applied recently to polymer solutions [28], for which the lack of local measurements within the channel required analytical treatments of the data. Nevertheless, the use of microviscometers on chip devoted to the study of complex fluids is a promising way.

The above considerations suppose a uniform dispersion of the particles within the carrier fluid and do not take into account lift forces. The role of lift forces generated in high aspect ratio microchannels has been studied recently [29,30]. The inertial migration of particles of diameter d dispersed in a liquid flowing through a straight channel will occur when $H<14d$. That condition was not satisfied by the microchannels and the nanofluids we have used, and we shall not consider the evolution of the equilibrium position of the particles furthermore.

III. NANOFLUIDS UNDER TEST AND EXPERIMENTAL DEVICES

Nanofluids with nine different monodisperse sizes SiO_2 particles, dispersed in ethanol, have been synthesized and tested. These nanofluids were synthesized following a colloidal route by Nano-H SAS. The silica nanoparticles were prepared from tetraethoxysilane in mixture of ammonia and ethanol. Hydrolysis and condensation reactions of the monomers tetraethoxysilane (TEOS) are summarized in Eqs. (6) and (7). The formation of the particles can be described on the following stages: depletion of alkoxide molecules followed by production of alcohol and formation of SiO_2,

$$\mathrm{Si(OC_2H_5)_4 + 4H_2O} \underset{\mathrm{EtOH}}{\overset{\mathrm{NH_4OH}}{\rightarrow}} \mathrm{Si(OH)_4 + 4C_2H_5OH}, \tag{6}$$

$$\mathrm{Si(OH)_4} \underset{\mathrm{EtOH}}{\overset{\mathrm{NH_4OH}}{\rightarrow}} \mathrm{SiO_2 \downarrow + 2H_2O}. \tag{7}$$

Controlled nanoparticles sizes can be achieved using an accurate concentration of reactives. In order to get particles with defined diameter stretching between 10 and 100 nm, the concentration of ammonia is situated typically between 8×10^{-2} and 8×10^{-1} mol L^{-1}, 0.3 mol^{-1} and 0.5 mol L^{-1} for TEOS, and 0 and 1.9 mol L^{-1} for water.

In a round bottom flask, alcohol, ammonia, and desionized water are stirred for few minutes. The TEOS monomer is added on the previous mixture and a white veil appears

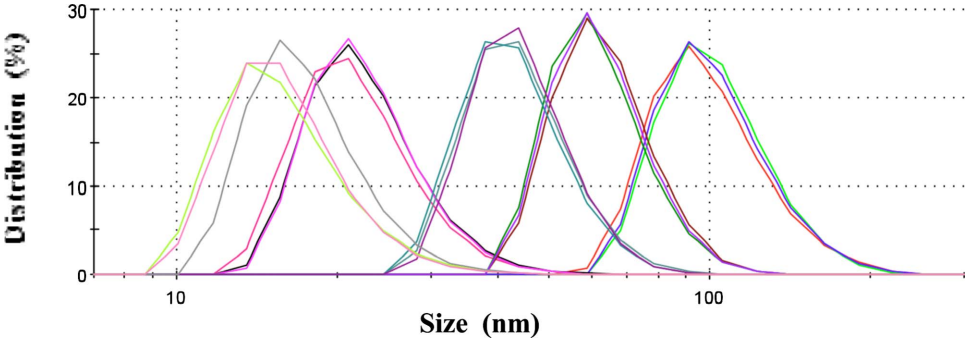

FIG. 2. (Color online) Particle size distributions histogram of silica nanobeads samples.

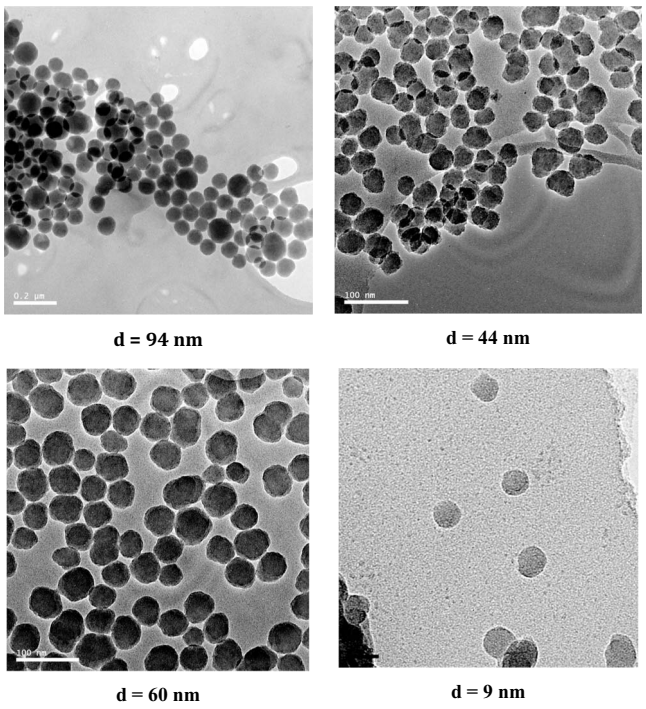

FIG. 3. TEM micrographs of 94, 60, 44, and 9 nm diameter SiO_2 nanoparticles.

after few minutes (more or less thick according to the nanoparticles size). Magnetic stirring was kept for 24 h at room temperature, the obtained silica nanobeads solution was dialyzed against ethanol using a cellulose membrane.

Dynamic light-scattering results were obtained using a He-Ne laser operating at 633 nm (Nano ZS Zetasizer, Malvern Instrument Ltd). Nanoparticles were dispersed in alcoholic solution.

The final size of the dispersed particles is controlled by laser granulometry (Fig. 2) and by TEM. A set of TEM micrographs is shown in Fig. 3. Nanoparticle size distribution is rather monodisperse. The average size of the silicon dioxide particles and the range of their solid volume concentrations are summarized in Table I. The volume fraction of the solid phase ϕ is calculated from the measured density ρ_{liq} of the base fluid ($\rho_{liq}=0.789$ g/cm^3) from the measured density ρ_{exp} of the nanofluid under test and from the density ρ_{sol} of the silicon dioxide nanoparticles ($\rho_{sol}=2.06$ g/cm^3) [31].

Our experiments were performed with hybrid silicon-Pyrex micromachined viscometers. The design of these devices allows to perform local pressure drops measurements ΔP over a length $L=10$ mm within the microchannel. The efficiency of these microsystems has been demonstrated by the past, by contributing to valid the laws of hydrodynamics at microscale [32]. The technical steps leading to the microfabrication of such microfluidic on chip viscometers and the experimental setup have been published elsewhere [33], and we shall not detail them. The use of these microchannels as capillary viscometers is founded on the measurement of the flow rate Q, related to the wall shear rate γ_w, and on the measurement of the pressure drop ΔP, related to the wall shear stress τ_w. For a Newtonian fluid, the dynamic viscosity η obeys $\eta=\tau_w/\gamma_w$ with

$$\gamma_w = \frac{6Q}{WH^2} \quad \text{and} \quad \tau_w = \frac{\Delta P}{L}\frac{H}{2}. \tag{8}$$

On one hand, the lowest H, the highest γ_w; on the other hand, the minimum value of γ_w is driven by the minimum accessible flow rate. We have performed microviscometers with $W=5$ mm and with 21 μm$<H<34$ μm. That range of heights is a balance between the above outlines. It is also a range of values that limit to a few seconds the hydraulic response time of the whole experimental loop. However, the minimum Q value is around 5 ml/h, and we had $\gamma_{min}\approx 2\times 10^3$ s^{-1}. So, unexpected low shear rate behaviors of the fluids under test, if any, are not measurable with these devices. Experimental uncertainties on γ_w are mainly the consequence of uncertainty on the height H of the microviscometer used; they were evaluated to 7%. The level of uncertainty on τ_w is the consequence of uncertainty on the pressure drop measurement and on the height H ($\approx$3%). Before each run, a measurement of the viscosity η_o of the base fluid was performed in order to take into account the influence of the temperature and to get a reliable value of the relative viscosity $\eta_{rel}=\eta/\eta_o$.

IV. RESULTS AND DISCUSSION

Preliminary results with shear rates up to $\gamma_w=5\times 10^4$ s^{-1} were performed onto nanofluids with $d=35$, 94, and 190 nm and have been published elsewhere [31]. We have completed the study with $d=9$, 11, 21, 22, 44, and 60 nm diameter nanoparticles and with shear rates ranging up to 2×10^5 s^{-1}. A selection of rheograms is plotted in Fig. 4. All the nanofluids have displayed a Newtonian behavior. No shear thinning nor shear thickening was observed for each individual nanofluid under test. As noticed above, we did not access to low shear rates, but the extension of the straight lines toward $\gamma_w->0$ indicates no evidence of a significant yield stress. For a given nanofluid, the highest ϕ, the highest η_{rel}. However, an anomalous enhancement of viscosity is observed with increasing volume concentration, as shown in Fig. 5. The conventional Einstein equation $\eta_{rel}=1+5\phi/2$ does not hold, even for low solid concentration. That is, the demonstration that the rheology of the nanofluids under test does not obey a model with individual spheres. The nonlinear evolution of $\eta_{rel}(\phi)$ is similar to the behavior of semiconcentrated suspensions. We can fit the viscosities to the

TABLE I. Range of the solid volume concentrations at which each nanofluid has been characterized.

d (nm)	9 ± 2	11 ± 2	21 ± 2	22 ± 2	35 ± 3	44 ± 3	60 ± 4	94 ± 5	190 ± 8
ϕ (%) min; max	0.7; 2.6	0.4; 7.3	2.6; 6.5	1; 6.2	1.3; 5.1	3.1; 7.1	3.1; 6.9	1.6; 7	1.1; 5.6

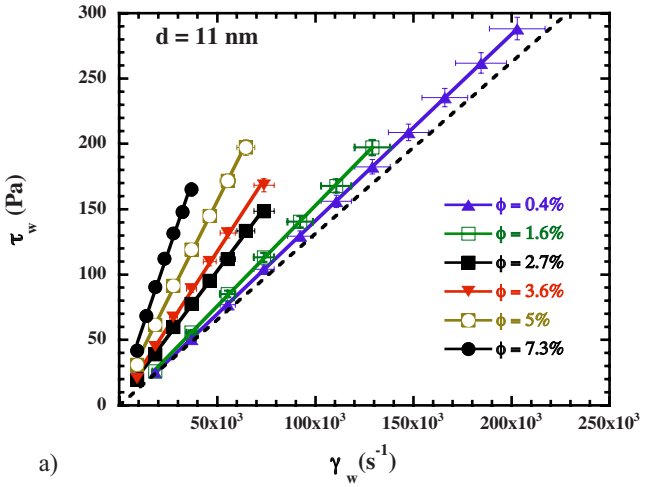

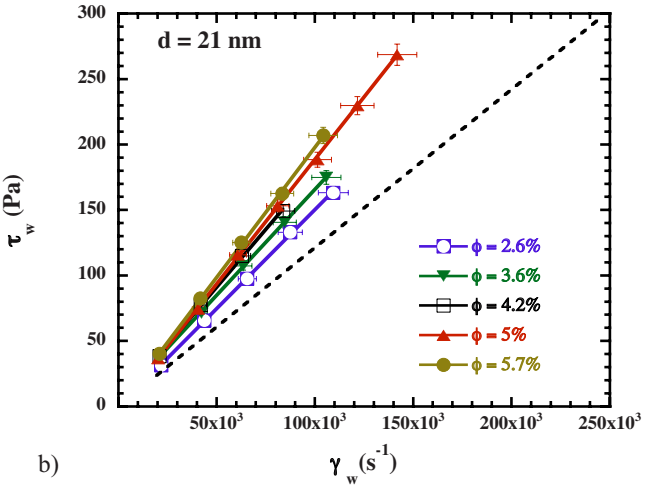

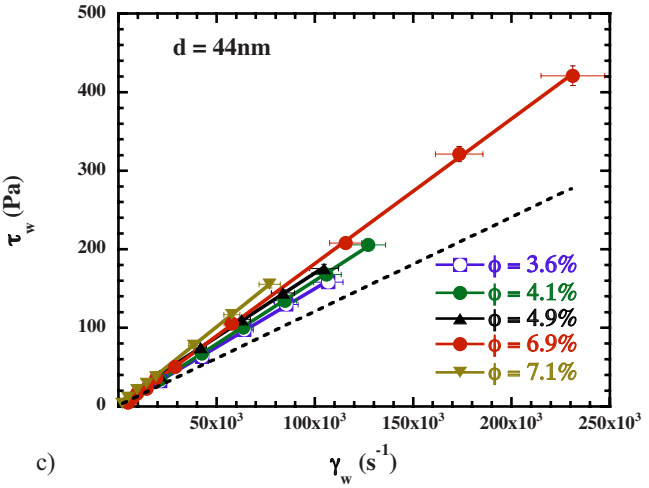

FIG. 4. (Color online) High shear rate rheograms of ethanol-based SiO_2 nanofluids at different solid volume concentrations with (a) $d=11$ nm, (b) $d=21$ nm, and (c) $d=44$ nm. The dashed line is the evolution of the base fluid without particles.

expression of Quemada [34] $\eta_{rel}=(1-\phi_a/\phi_m)^{-2}$, where ϕ_m is the crowding factor ($\phi_m \approx 0.65$ for random packing of spheres) and ϕ_a is an apparent solid volume fraction. The fact that there is an anomalous size effect means that $\phi_a = \phi_a(d)$ and is consistent with the presence of aggregates

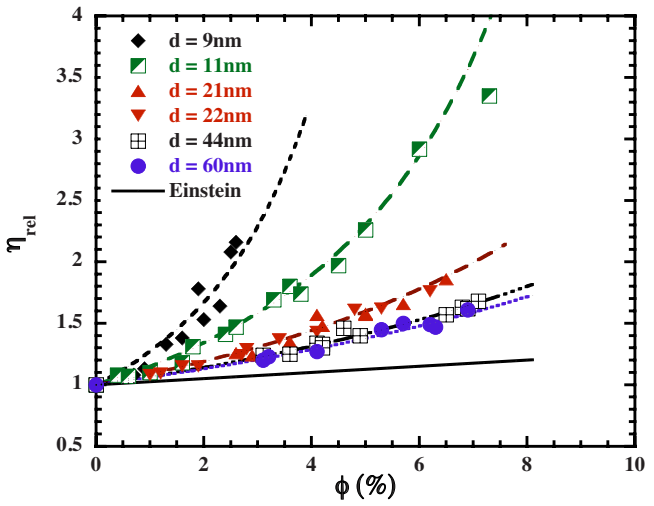

FIG. 5. (Color online) Evolution of the relative viscosity of SiO_2-ethanol nanofluids as a function of the volume concentration. The anomalous enhancement of the viscosity and the particle-size effect are a consequence of both aggregates size and hydrodynamic interactions. The values, which are above the classical model of Einstein for individual particles, agree with Eq. (9) (dashed plots).

[35]. The volume fraction of the aggregates of average diameter D_a is $\phi_a=\phi(D_a/d)^{3-d_f}$, where $d_f \approx 1.8$ is the fractal dimension, which is assumed to accord to a diffusion-limited cluster-cluster aggregation model for nanofluids [35]. As a consequence, the viscosities obey

$$\eta = \eta_0\left[1-\frac{\phi}{\phi_m}\left(\frac{D_a}{d}\right)^{1.2}\right]^{-2}. \tag{9}$$

The experimental results in Fig. 5 are fitted with Eq. (9). It becomes possible to calculate, for each nanofluid, the ϕ_a/ϕ ratio, an average diameter D_a of aggregates and an

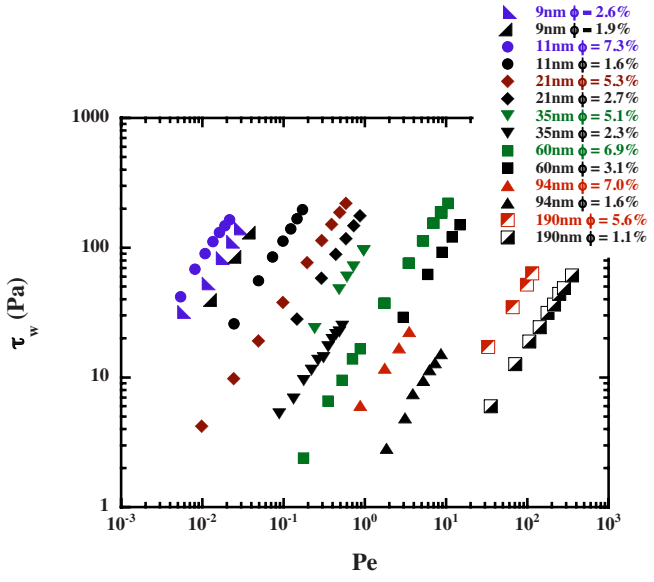

FIG. 6. (Color online) Selection of the evolution of the wall shear stress of different nanofluids versus the adimensional Pe number.

TABLE II. Ratio of the apparent on the real solid concentration, calculation of the average diameter D_a of the aggregates, and of the number N_a of nanoparticles within the aggregates for each nanofluid.

d (nm)	9	11	21	22	35	44	60	94	190
ϕ_a/ϕ	7.45	4.50	2.75	2.75	3.60	2.10	1.95	2.50	2.20
D_a (nm)	48	39	49	49	102	82	105	202	367
N_a	20	10	5	5	7	3	3	4	3

average number of particles $N_a=(D_a/d)^{1.8}$ within a single aggregate [35]. These values are reported in Table II. A decrease in N_a and ϕ_a/ϕ is observed as d increases. However, a shift between the set of results obtained with the nanofluids previously tested ($d=35$, 94, and 190 nm) and those obtained from experiments performed under very high shear rates ($d=9$, 11, 21, 22, 44, and 60 nm) is clearly noticeable. We believe that it is the consequence of strong shearing forces and of Pe values at which the experiments were performed, respectively, as displayed in Fig. 6. Each nanofluid, at fixed solid volume concentration, has been characterized over two orders of magnitude of the Pe number, and only the lower and higher edges covered by Pe have been reported in Fig. 6. Unfortunately, it was not experimentally possible to cover a broader range of Pe values and to enhance a variation in the viscosity, if any, for one fixed nanofluid. However, the set of data run from $\mathrm{Pe}=5\times10^{-3}$ to $\mathrm{Pe}=350$, and the conditions $\mathrm{Pe}<1$, $\mathrm{Pe}\approx1$, and $\mathrm{Pe}>1$ have been scrutinized.

The data obtained with $d=9$ and 11 nm obey $\mathrm{Pe}\ll1$; the results are then consistent with Fig. 1(a): the Brownian motion enhances the formation of aggregates of approximately four times the primary nanoparticle size.

As Pe and the upper limit of the wall shear stress increase, the ratio ϕ_a/ϕ decreases: the average diameter D_a becomes around twice the basic particle size, that is, consistent with Fig. 1(b). The strong shearing forces affect the size and the aspect ratio of the agglomerates with an intensity, which depends on the diameter of the nanoparticles. A question arises, to know whether the strong shearing force can deeply affect the spherical shape of the clusters, by giving way to the formation of monolayers or to the formation of trains of particles. As the width W of the microviscometers is always high before the height H, the formation of long stripes of particles is unlikely. The formation of monolayers including a limited number of particles, when $\mathrm{Pe}>1$, seems to be a more relevant hypothesis, in such an experimental configuration.

The $d=190$ nm nanofluid was tested in the range $17<\mathrm{Pe}<350$ and no shear thickening effect was observed. That means that orthokinetic aggregation did not occur with the nanofluids under test. That is still coherent with the assumption that monolayers of nanoparticles flow on stratified planes, with low interactions.

V. CONCLUSIONS

We have presented an experimental study of the rheology of silicon dioxide nanofluids submitted to strong shear rates. The strong enhancement of the viscosity of these suspensions, with increasing their volume concentration, agrees with the presence of aggregates. Moreover, an average aspect ratio of the aggregates could be drawn for each set of nanofluids. It has been demonstrated that the mean number of nanoparticles within the aggregates strongly depends on the hydrodynamic interactions. Strong shearing forces are assumed to affect the aspect ratio of the aggregates. The effects of these interactions are more pronounced for large nanoparticles owing higher Pe values. In that case, our results are consistent with a configuration, where clusters have been thinned in small aggregates, each of them containing a few particles. Such an experimental evidence of the presence and of the structure of aggregates in nanofluids is a contribution to a better understanding of their thermal properties.

ACKNOWLEDGMENTS

This work took advantage of the technical pools of the Néel Institute. The Nanofab facilities allowed the machining of the microviscometers on chip. The electronic pool of the MCBT Department gave us helpful assistance. M. Bacia is greatly acknowledged for having performed the TEM micrographs.

[1] P. Keblinski, R. Prasher, and J. Eapen, J. Nanopart. Res. **10**, 1089 (2008).
[2] W. Evans, R. Prasher, J. Fish, P. Meakin, P. Phelan, and P. Keblinski, Int. J. Heat Mass Transfer **51**, 1431 (2008).
[3] J. Eapen, W. C. Williams, J. Buongiorno, L. W. Hu, S. Yip, R. Rusconi, and R. Piazza, Phys. Rev. Lett. **99**, 095901 (2007).
[4] J. Philip, P. D. Shima, and B. Raj, Appl. Phys. Lett. **91**, 203108 (2007).
[5] S. M. Sohel Murshed, J. Nanopart. Res. **11**, 511 (2009).
[6] A. J. Schmidt, M. Chiesa, D. H. Torchinsky, J. A. Johnson, A. Boustani, G. H. McKinley, K. A. Nelson, and G. Chen, Appl. Phys. Lett. **92**, 244107 (2008).
[7] R. Prasher, D. Song, J. Wang, and P. Phelan, Appl. Phys. Lett. **89**, 133108 (2006).
[8] E. V. Timofeeva, A. N. Gavrilov, J. M. McCloskey, Y. V. Tolmachev, S. Sprunt, L. M. Lopatina, and J. V. Selinger, Phys. Rev. E **76**, 061203 (2007).
[9] S. K. Das, N. Putra, and W. Roetzel, Int. J. Heat Mass Transfer

46, 851 (2003).
[10] J. Garg, B. Poudel, M. Chiesa, J. B. Gordon, J. J. Ma, J. B. Wang, Z. F. Ren, Y. T. Kang, H. Ohtani, J. Nanda, G. H. McKinley, and G. Chen, J. Appl. Phys. **103**, 074301 (2008).
[11] S. M. S. Murshed, K. C. Leong, and C. Yang, Int. J. Therm. Sci. **47**, 560 (2008).
[12] S. M. S. Murshed, K. C. Leong, and C. Yang, Appl. Therm. Eng. **28**, 2109 (2008).
[13] H. Chen, Y. Ding, and C. Tan, New J. Phys. **9**, 367 (2007).
[14] W. J. Tseng and K.-C. Lin, Mater. Sci. Eng., A **355**, 186 (2003).
[15] K. Kwak and C. Kim, Korea-Aust. Rheol. J. **17**, 35 (2005).
[16] Y. He, Y. Jin, H. Chen, Y. Ding, D. Cang, and H. Lu, Int. J. Heat Mass Transfer **50**, 2272 (2007).
[17] H. Chen, Y. Ding, Y. He, and C. Tan, Chem. Phys. Lett. **444**, 333 (2007).
[18] Y. S. Lee and N. Wagner, Ind. Eng. Chem. Res. **45**, 7015 (2006).
[19] A. R. Studart, E. Amstad, M. Antoni, and L. J. Gauckler, J. Am. Ceram. Soc. **89**, 2418 (2006).
[20] L. Vekas, Rom. J. Physiol. **49**, 707 (2004).
[21] Y. Yang, E. A. Grulke, Z. G. Zhang, and G. Wu, J. Appl. Phys. **99**, 114307 (2006).
[22] G. H. Ko, K. Heo, K. Lee, D. S. Kim, C. Kim, Y. Sohn, and M. Choi, Int. J. Heat Mass Transfer **50**, 4749 (2007).
[23] J. Liao, Y. Zhang, W. Yu, L. Yu, C. Ge, J. Liu, and N. Gu, Colloids Surf., A **223**, 177 (2003).
[24] P. Meakin, Phys. Rev. Lett. **51**, 1119 (1983).
[25] D. A. Weitz and M. Oliveria, Phys. Rev. Lett. **52**, 1433 (1984).
[26] D. R. Foss and J. F. Brady, J. Fluid Mech. **407**, 167 (2000).
[27] M. Kamibayashi, H. Ogura, and Y. Otsubo, J. Colloid Interface Sci. **321**, 294 (2008).
[28] K. Kang, L. J. Lee, and K. W. Koelling, Exp. Fluids **38**, 222 (2005).
[29] A. A. S. Bhagat, S. S. Kuntaegowdanahalli, and I. Papautsky, Phys. Fluids **20**, 101702 (2008).
[30] D. Di Carlo, D. Irimia, R. G. Tompkins, and M. Toner, Proc. Natl. Acad. Sci. U.S.A. **104**, 18892 (2007).
[31] J. Chevalier, O. Tillement, and F. Ayela, Appl. Phys. Lett. **91**, 233103 (2007).
[32] R. Bavière, F. Ayela, S. Leperson, and M. Favre-Marinet, Phys. Fluids **17**, 098105 (2005).
[33] J. Chevalier and F. Ayela, Rev. Sci. Instrum. **79**, 076102 (2008).
[34] D. Quemada, Rheol. Acta **16**, 82 (1977).
[35] R. Prasher, P. E. Phelan, and P. Bhattacharya, Nano Lett. **6**, 1529 (2006).